Netsu Sokutei **30** (2) 76-84

解　説

Excess Thermodynamic Functions of Binary Liquid Mixtures Using Rayleigh Laser Light Scattering

Gerald R. Van Hecke and Robert A. Westervelt

(Received February 10, 2003; Accepted March 4, 2003)

Rayleigh light scattering ratios obtained using a laser light source, combined with molar volume and refractive index measurements, were used to evaluate the excess Gibbs potentials of mixing in binary liquid mixtures. When these quantities are measured as functions of temperature, as well as composition, the excess enthalpy and entropy of the binary mixtures can be obtained. This contribution presents the pertinent experimental techniques and data analyses necessary to extract excess Gibbs potentials from light scattering measurements. Data is presented for one representative system consisting of toluene and propan-2-ol mixtures.

1. Introduction

Thermodynamic data for binary liquid mixtures has been traditionally obtained from vapor-liquid equilibria and calorimetry measurements. However, light scattering techniques can also be used to obtain thermodynamic information. For instance, Rayleigh light scattering has long been extensively used to measure second virial coefficients in polymer solutions. Another procedure using laser light scattering provides a method to measure solvent-solvent interactions thereby providing a direct method of quantifying the excess Gibbs potential for a binary liquid mixture. For example, Coumou and Mackor used light scattering to measure the excess Gibbs potential in binary mixtures of benzene and various hydrocarbons.[1] Until recently light scattering measurements on binary mixtures used a mercury lamp light source.[2,3,4] The availability of lasers with more than adequate intensity, greatly increases the ease of experimentation with improved precision as well. Even though several independent measurements are necessary to use the light scattering technique, measurements as functions of temperature are very convenient and allow the ready estimation of excess entropies and enthalpies from the excess Gibbs potentials.

2. Theory

Light scattering data are most often discussed in terms of Rayleigh ratios to avoid the necessity of measuring absolute intensities. Early light scattering measurements used un-polarized light. Most lasers are polarized which means the treatments in terms of un-polarized light need to be modified for polarized light. This is done below. For un-polarized incident light, the total Rayleigh ratio can be written as the sum of an isotropic and an anisotropic term yielding

$$R_{\mathrm{TOT,U}}(\theta)=R_{\mathrm{IS}}(\theta)+R_{\mathrm{AN}}(\theta) \tag{1}$$

where the subscripts 'IS' and 'AN' denote an isotropic term due to concentration as well as density fluctuations and an anisotropic term due to orientation fluctuations respectively.

Cabbanes suggested a way of separating R_{IS} and R_{AN} from the measured total Rayleigh ratio by taking into account the polarizations of the scattered light.[5] He suggested that

$$R_{\mathrm{IS}}(90)=R_{\mathrm{TOT,U}}(90)\left[\frac{6-7\rho_{\mathrm{U}}(90\ ^{\circ})}{6+7\rho_{\mathrm{U}}(90\ ^{\circ})}\right] \tag{2}$$

where $\rho_{\mathrm{U}}(90\ ^{\circ})$ is the polarization ratio for incident un-polarized light measured at 90 $^{\circ}$ from the incident light

$$\rho_U(90^\circ) = \left(\frac{I_H}{I_V} \right) \tag{3}$$

Here I_V and I_H are the vertical and horizontal components of the light scattered at 90° respectively. Extending this concept to incident polarized light gives

$$\rho_U(90^\circ) = \left(\frac{I_{HV} + I_{HH}}{I_{VV} + I_{VH}} \right) \tag{4}$$

where I_{XY} stands for the intensity of the light scattered at 90° where the incident beam is polarized X (either (H)orizontally or (V)ertically) and the scattered beam is detected polarized Y (H or V).
Since at 90° $I_{VH} = I_{HV} = I_{HH}$,[6]

$$R_{IS}(90) = R_{TOT,U}(90) \left[\frac{3I_{VV} - 4I_{VH}}{3I_{VV} - 9I_{VH}} \right] \tag{5}$$

Thus, the isotropic component of the total Rayleigh ratio is experimentally accessible from the measured intensities of the scattered polarized light and the total Rayleigh ratio.

For incident polarized light, $R_{TOT,U}$ taking into account the various components of the polarized light is given by

$$R_{TOT,U} = \frac{1}{2} (R_{VV} + 3R_{HH}) \tag{6}$$

where R_{VV} and R_{VH} are the total Rayleigh ratios for vertically vertical and vertically horizontal polarized scattered light respectively.[6-8] This expression also takes advantage of the fact that at 90° $I_{VH} = I_{HV} = I_{HH}$.

Experimentally all of the intensities are calibrated to some standard. Cohen and Eisenberg also suggested a calibration factor to take into account the refractive index of each solution[2] yielding

$$R_{TOT,U} = \frac{1}{2} \left[R_{VV,STD} \left(\frac{I_{VV}}{I_{VV,STD}} \right) + 3R_{HHSTD} \left(\frac{I_{VH}}{I_{VH,STD}} \right) \right] \left(\frac{n}{n_{STD}} \right)^2 \tag{7}$$

Thus, R_{IS} and $R_{TOT,U}$ may be calculated from measured I_{VV}, I_{VH}, and the refractive index n for each sample and the standard measured at the wavelength of the laser. Calibration is achieved using a literature value for R_{VVSTD}. Toluene served not only as the literature standard in our studies but also one of the components of our studied mixtures.

Einstein demonstrated that the isotropic component, R_{IS}, of the total Rayleigh ratio was proportional to the square of fluctuations in the dielectric constant for a given sample.[9] For mixtures, fluctuations occur in both the density and the concentration in a given sample. Thus, R_{IS} can be subdivided into terms representing contributions of density fluctuations, R_D, concentration fluctuations, R_C, and a coupling term R_{DC}. allowing for the interdependence of R_D and R_C. This gives

$$R_{IS} = R_D + R_C + R_{DC} \tag{8}$$

While R_{DC} is generally small, as it was in these experiments (*vide infra*), its contribution should not be neglected a priori. In fact Brown *et al.*[10] found R_{DC} to be quite significant in their studies of a variety of hydrocarbon mixtures.

The first expression for R_D was developed by Einstein[9] as

$$R_D = \left(\frac{\pi^2}{2\lambda^4} \right) k_B T \kappa_T \left[N \left(\frac{\partial \varepsilon}{\partial N} \right)_T \right]^2 \tag{9}$$

where λ is the wavelength of incident light, k_B is Boltzmann's constant, T is the absolute temperature, κ_T is the isothermal compressibility of the solution, and N is the number density of the solution.

For the coupling term the results of Šegudović and Deželić[8] give

$$R_{DC} = \left(\frac{\pi^2}{2\lambda^4} \right) k_B T \kappa_T X_1 X_2 \left[N \left(\frac{\partial \varepsilon}{\partial N} \right)_T \right] \left(\frac{\partial \varepsilon}{\partial X_2} \right)_T \tag{10}$$

Both R_D and R_{DC} contain the term $(\partial \varepsilon / \partial N)_T$. The evaluation of this derivative has been the subject of consideration discussion and there are at least three ways to estimate the derivative: using the Lorenz-Lorentz equation, using the empirical Eykman approximation, or using piezo-optic coefficients. The Eykman approximation will be used here.[11] In this approximation $(\partial \varepsilon / \partial N)_T$ is

$$N \left(\frac{\partial \varepsilon}{\partial N} \right)_T = \frac{2n(n + 0.4)(n^2 - 1)}{(n^2 + 0.8n + 1)} \tag{11}$$

Substituting the Eykman approximation into R_D and R_{DC} gives

$$R_D = \left(\frac{\pi^2}{2\lambda^4}\right) k_B T \kappa_T \left[\frac{2n(n+0.4)(n^2-1)}{(n^2+0.8n+1)}\right]^2$$

$$R_{DC} = \left(\frac{\pi^2}{2\lambda^4}\right) k_B T \kappa_T X_1 X_2 \left[\frac{2n(n+0.4)(n^2-1)}{(n^2+0.8n+1)}\right]\left[2n\left(\frac{\partial n}{\partial X_2}\right)_T\right] \quad (12)$$

In the expressions for R_D and R_{DC}, n^2 was substituted for ε which is a valid approximation at the optical frequencies of the visible laser light. In equations (10) and (12), X_1 and X_2 are the mole fractions of components 1 and 2 of the mixture.

The expressions for R_D and R_{DC} both involve κ_T as a function of composition. Many workers[3,8] use a density weighted linear combination of the pure component compressibilities to obtain κ_T for mixtures (see below). In fact several authors use the light scattering of the pure materials to calculate κ_T [8,10,12,13]

The composition dependent R_C can be obtained "experimentally" by subtracting R_D and R_{DC} from R_{IS} using equation (8). Theoretically, R_C is given by

$$R_C = \left(\frac{2\pi^2}{\lambda^4}\right) k_B T V X_1 \left[\frac{n^2\left(\frac{\partial n}{\partial X_2}\right)^2}{\left(\frac{\partial \mu_2}{\partial X_2}\right)}\right] \quad (13)$$

where V is the molar volume of the solution. The partial derivative of chemical potential μ_2 with respect to composition contains the desired thermodynamic information.

For an ideal solution,

$$R_{C,ID} = \left(\frac{2\pi^2}{\lambda^4}\right)\left(\frac{VX_1X_2}{N_A}\right)\left[n^2\left(\frac{\partial n}{\partial X_2}\right)^2\right] \quad (14)$$

For non-ideal solutions,

$$\frac{\partial \mu_2}{\partial X_2} = \frac{N_A k_B T}{X_2} - (1-X_2)\left(\frac{\partial^2 G^E}{\partial X_2^2}\right) \quad (15)$$

Combining equations (13), (14) and (15)

$$\left[\frac{R_{C,ID}}{R_C} - 1\right] = \frac{X_1 X_2}{N_A k_B T}\left(\frac{\partial^2 G^E}{\partial X_2^2}\right) \quad (16)$$

Equation (16) connects the excess Gibbs potential, the desired thermodynamic quantity, to $R_{C,ID}$ and R_C which are in turn determined by the extent of fluctuations in concentration and density. The presence of non-zero intermolecular interactions affects the magnitude of these fluctuations and hence the magnitude of R_C.

Some functional form is required for the excess Gibbs potential. One approach is the Flory-Huggins theory[14,15] which casts the data in terms of volume fraction. We chose to analyze the data using the empirically derived Redlich-Kister polynomial expansion written in terms of mole fraction[16]

$$G^E = X_1 X_2 \sum_{J=1}^{n} g_J (1-2X_2)^{J-1} \quad (17)$$

Here the g_J parameters are assumed to only depend on temperature and pressure and are determined by a least squares fit to the $\partial^2 G^E/\partial x^2$ data. Suppose G^E is fit to an n^{th} order Redlich-Kister polynomial. Then the $\partial^2 G^E/\partial x^2$ function will fit to an (n-2) order polynomial. However, differentiating the Redlich-Kister polynomial twice with respect to X_2 has the important feature of not losing or scrambling any of the g_J coefficients. Thus the coefficients for the n^{th} order fit to G^E can be obtained from a least squares fit to the (n-2) order Redlich-Kister polynomial used to fit the $\partial^2 G^E/\partial x^2$ data. Another advantage of the Redlich-Kister polynomial is the thermodynamic consistency it provides for G^E since it satisfies the Gibbs-Duhem equation.

3. Experimental Section

Determining the excess Gibbs potential for binary liquid mixtures by light scattering entails the measurement of three quantities each as a function of composition and temperature: light scattering intensity, density, and refractive index. We use isothermal compressibility values calculated from the R_D of the pure components.

4. Sample preparation

Reagent grade toluene (Aldrich) was fractionally distilled, filtered using a 0.22 micron Millipore frit, and degassed by additional boiling. Aldrich HPLC grade propan-2-ol was fractionally distilled over CaH_2, filtered using a 0.22 micron Millipore frit, and degassed by boiling. All solutions were prepared by weighing each component without buoyancy correction.

5. Laser light scattering

The light scattering measurements were made using

Table 1 Light scattering intensity at 488 nm in units of 10^{-6} amps for mixtures of propan-2-ol and toluene measured at 288, 298, 308, and 318 K. Composition is given as mole fraction of toluene. Vertical incident, vertically detected light is noted as I_{VV}. Vertical incident, horizontally detected light is noted as I_{VH}.

	288 K		298 K		308 K		318 K	
$X_{toluene}$	$I_{VV}/10^{-6}$ a	$I_{VH}/10^{-6}$ a	$I_{VV}/10^{-6}$ a	$I_{VH}/10^{-6}$ a	$I_{VV}/10^{-6}$ a	$I_{VH}/10^{-6}$ a	$I_{VV}/10^{-6}$ a	$I_{VH}/10^{-6}$ a
0.0000	1.88±0.13	0.0572±0.004	1.89±0.014	0.079±0.002	3.26±0.06	0.089±0.004	3.97±0.16	0.009±0.005
0.0947	3.32±0.11	0.246±0.005	3.17±0.042	0.231±0.008	5.01±0.14	0.241±0.004	5.52±0.26	0.255±0.011
0.2089	4.62±0.21	0.447±0.017	4.37±0.048	0.426±0.010	6.16±0.14	0.403±0.014	6.32±0.25	0.444±0.013
0.2905	5.85±0.17	0.594±0.014	5.30±0.044	0.550±0.000	8.21±0.14	0.524±0.010	7.33±0.25	0.597±0.011
0.4020	7.33±0.20	0.761±0.022	6.68±0.15	0.717±0.019	8.53±0.29	0.665±0.019	7.42±0.17	0.768±0.010
0.5075	8.30±0.19	0.913±0.013	7.48±0.046	0.891±0.011	8.73±0.22	0.779±0.025	7.91±0.01	0.925±0.010
0.6087	9.08±0.26	1.09±0.028	9.90±0.074	1.01±0.010	10.03±0.35	0.945±0.039	8.46±0.27	1.11±0.039
0.7044	8.06±0.06	1.25±0.010	6.72±0.16	1.09±0.021	8.32±0.15	1.065±0.017	7.29±0.31	1.23±0.059
0.7932	6.73±0.28	1.32±0.038	5.96±0.11	1.20±0.026	7.89±0.09	1.19±0.019	7.03±0.20	1.36±0.041
0.9279	4.85±0.31	1.43±0.090	4.61±0.006	1.34±0.006	6.26±0.13	1.29±0.034	6.05±0.21	1.45±0.050
1.0000	4.30±0.08	1.52±0.034	3.82±0.010	1.38±0.006	5.51±0.21	1.38±0.049	5.18±0.01	1.52±0.006

a modified Brice-Phoenix scattering photometer. The sample cell consisted of a 1" diameter precision bore tubing approximately 1.5" long. The base of the sample cell was a piece of flat glass attached to the tubing using GE silicone cement. About 5 mL of solution were placed in the cell.

The 488 nm line of a Coherent Nova 70 argon ion laser was used. The power level was approximately 80 mW after being passed through a 1.0 OD neutral density filter. The actual power was maintained at a constant level by periodically checking the power level with a Coherent Model 200 power meter. A broadband polarization rotator was placed directly outside the photometer to change the polarization of the incident beam. The PMT housing was modified to allow the placement of a polaroid sheet and a 488 nm interference filter between the sample and the detector. The scattering intensities were made by rotating the incident beam between vertical and horizontal polarizations and while keeping the polaroid sheet in front of the detector in a vertical position. All scattering measurements were taken at an angle of 90 ° from the incident beam. The temperature of the samples was maintained through the use of a thermostated circulating bath. Temperature control was considered to be ±0.5 ℃. Great care was taken to place the cell reproducibly in the scattering chamber. The raw light scattering intensities are tabulated in **Table 1** and represent at least 4 replicate measurements based on removing the cell, repositioning and rereading.

The detector consisted of an air cooled PMT. The signal from the PMT was fed directly into a Keithley picoammeter. Dark currents were initially measured but proved insignificant compared to the magnitudes of the signals generated.

Toluene was used as Rayleigh ratio the calibration standard. The value for R_V for toluene was taken to be 9.780×10^{-4} m^{-1} at 690 nm and 25 ℃ as suggested by Wyatt Technologies based on the work of Kaye and McDaniel.[17] The R_V at 488 nm was calculated to be 39.09×10^{-4} m^{-1} using the λ^4 factor. R_{VV} and R_{HH} which are necessary to use equation (7) are found using equations (18).

$$R_{VVSTD} = R_{VSTD}\left[\frac{1+\rho_{USTD}}{1+3\rho_{USTD}}\right]$$
$$R_{HHSTD} = R_{VVSTD}\left[\frac{\rho_{USTD}}{2-\rho_{USTD}}\right] \quad (18)$$

For other temperatures (℃), $R_{VV}(t)$ is found from $R_{VV}(t) = R_{VV}(25)[1+0.00368(t-25\,℃)]$.[18]

6. Density measurements

The solution densities were determined at several temperatures using an Anton Parr Model DMA40 density meter calibrated using literature values for pure propan-2-ol, and toluene. **Table 2** contains the densities as functions of temperature and composition for the propan-

Table 2 Densities in units of g/mL and refractive indices at 488 nm for mixtures of propan-2-ol and toluene at 288, 298, 308, and 318 K. The uncertainty in density is ±0.0005 g/mL. Composition is mole fraction of toluene. The difference between n_{488} and n_{589} is the dispersion correction, the change in refractive index from the traditional 589 nm sodium D line index to that measured at the Argon ion laser line at 488 nm. The uncertainty in the refractive indices is ±0.0002.

	288 K			298 K			308 K			318 K		
$X_{toluene}$	ρ_{288}	n_{488}	n_{589}	ρ_{298}	n_{488}	n_{589}	ρ_{308}	n_{488}	n_{589}	ρ_{318}	n_{488}	n_{589}
0.0000	0.7892	1.3908	1.3779	0.7814	1.3877	1.3740	0.7738	1.3832	1.3695	0.7664	1.3789	1.3655
0.0947	0.8001	1.4073	1.3916	0.7916	1.4033	1.3892	0.7836	1.3984	1.3840	0.7757	1.3939	1.3802
0.2089	0.8118	1.4253	1.4100	0.8028	1.4208	1.4051	0.7944	1.4156	1.4004	0.7859	1.4107	1.3960
0.2905	0.8194	1.4371	1.4212	0.8101	1.4325	1.4165	0.8015	1.4271	1.4112	0.7928	1.4220	1.4066
0.4020	0.8290	1.4520	1.4353	0.8195	1.4474	1.4305	0.8106	1.4418	1.4250	0.8016	1.4365	1.4200
0.5075	0.8372	1.4650	1.4477	0.8277	1.4604	1.4425	0.8166	1.4549	1.4370	0.8094	1.4493	1.4320
0.6087	0.8446	1.4767	1.4577	0.8352	1.4722	1.4536	0.8258	1.4666	1.4480	0.8166	1.4609	1.4430
0.7044	0.8513	1.4872	1.4692	0.8419	1.4828	1.4638	0.8325	1.4771	1.4581	0.8232	1.4714	1.4530
0.7932	0.8573	1.4966	1.4758	0.8480	1.4922	1.4727	0.8385	1.4864	1.4670	0.8292	1.4807	1.4618
0.9279	0.8665	1.5017	1.4907	0.8572	1.5058	1.4858	0.8478	1.4998	1.4800	0.8384	1.4942	1.4751
1.0000	0.8716	1.5182	1.4981	0.8622	1.5128	1.4925	0.8528	1.5066	1.4858	0.8434	1.5012	1.4810

2-ol / toluene system. Temperature variation and control were provided by a circulating thermostated bath and good to ±0.1 ℃.

7. Refractive index measurements

The refractive index measurements were taken at the sodium-D line 589 nm with a Bausch and Lomb Abbe' Model 3 refractometer. Temperature variation and control were provided by a circulating thermostated bath and good to ±0.1 ℃. The instrument was calibrated with absolute ethanol and a dispersion correction was made to 488 nm following the manufacturer's instructions. Since no absorption bands are observed in the range from 589 nm to 488 nm the dispersion should not be large or vary widely. The dispersion correction ranged from ～ 0.01 to ～ 0.004. The refractive indices at the 589 nm and 488 nm are also given in **Table 2**.

8. Isothermal Compressibilities

Equation (12) for R_D has been used to calculate isothermal compressibilities for pure liquids.[10,12,13] The only assumption in equation (12) is the validity of the Eykman approximation. We have used this approach and calculated κ_T for propan-2-ol and toluene at each of the measured temperatures directly from the light scattering and refractive index data. **Table 3** presents the calculated κ_T at 288, 298, 308, and 318 K.

Table 3 Isothermal compressibilities κ_T for the pure components at 288, 298, 308, and 318 K. Table entries should be multiplied by 10^{-10} Pa^{-1}.

Substance	288 K	298 K	308 K	318 K
Toluene	7.5±1.7	7.6±0.3	11.0±3.6	10.0±0.2
Propan-2-ol	10.7±3.5	12.2±0.4	16.8±1.6	22.4±4.0

Binary solution isothermal compressibilities were calculated using equation (19).

$$\kappa_T = \rho\left[\frac{(1-X_2)\kappa_{T1}}{\rho_1} + \frac{(X_2)\kappa_{T2}}{\rho_2}\right] \qquad (19)$$

where ρ, ρ_1, and ρ_2 are the densities of the solution and pure components 1 and 2 respectively and X_2 is the mole fraction of component 2.

9. Data Analysis

All of the calculations and plots were done using Axum 6.0 or MathCad 2000 software by MathSoft.

10. Results and Discussion

The Rayleigh ratios R_{IS}, R_D, R_{DC}, R_C, $R_{C,ID}$ at the four temperatures studied are presented in **Fig.1**. The supporting data for the 288 K Rayleigh ratios is given

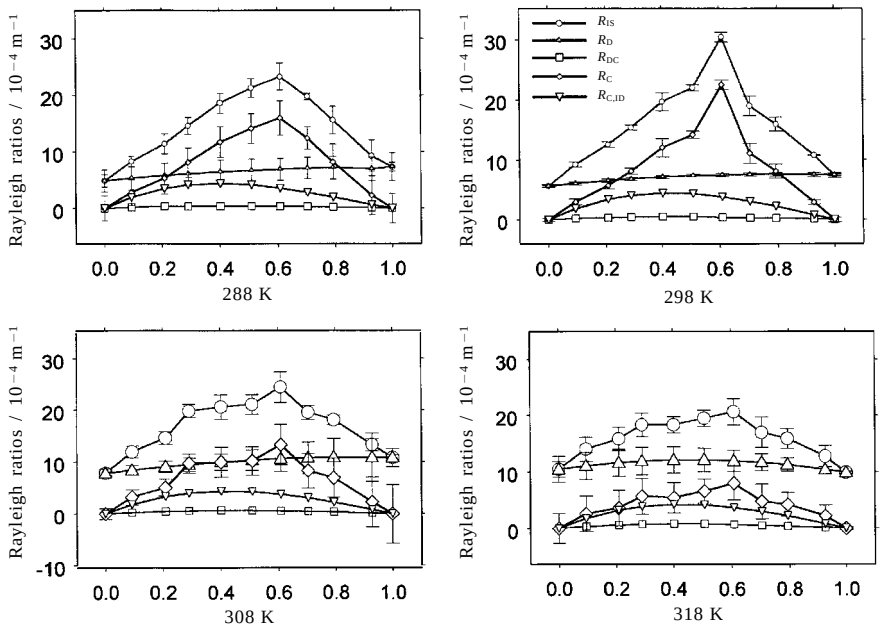

Fig.1 Rayleigh ratios in terms of 10^{-4} m^{-1} at 288, 298, 308, and 318 K. R_{IS} =○, R_D =△, R_{DC} =□, R_C =◇, $R_{C,ID}$ =▽. Composition is mole fraction of toluene. Uncertainties were estimated using addition in quadrature of the uncertainties in the experimental factors. Lines are drawn for ease of distinguishing plots and do not represent any data fitting.

Table 4 Rayleigh ratio results at 288 K for mixtures of propan-2-ol and toluene. Composition is mole fraction of toluene. The uncertainty in R_{DC} is not significant and the values of $R_{C,ID}$ are taken as standard values without uncertainty. The magnitudes of $\partial^2 G^E/\partial X^2$ approach negative infinity as $X_{toluene}$ approaches 0 or 1.

$X_{toluene}$	$R_{TOT}/(10^{-4}$ m$^{-1})$	$R_{IS}/(10^{-4}$ m$^{-1})$	$R_D/(10^{-4}$ m$^{-1})$	$R_{DC}/(10^{-4}$ m$^{-1})$	$R_C/(10^{-4}$ m$^{-1})$	$R_{C,ID}/(10^{-4}$ m$^{-1})$	$\partial^2 G^E/\partial X^2$/(kJ mol^{-1})
0.0000	5.56 ± 0.37	4.90 ± 1.10	4.90 ± 1.96	0	0	0	—
0.0947	11.27 ± 0.36	8.32 ± 0.92	5.35 ± 2.06	0.17	2.80 ± 2.26	1.96	−8.37 ± 15.8
0.2089	16.99 ± 0.67	11.47 ± 1.77	5.82 ± 2.13	0.32	5.33 ± 2.77	3.53	−4.91 ± 5.0
0.2905	22.12 ± 0.61	14.66 ± 1.46	6.12 ± 2.13	0.38	8.16 ± 2.59	4.15	−5.71 ± 1.9
0.4020	28.44 ± 0.77	18.69 ± 1.77	6.48 ± 2.09	0.42	11.79 ± 2.74	4.42	−6.23 ± 0.9
0.5075	33.24 ± 0.78	21.33 ± 1.70	6.74 ± 2.02	0.41	14.18 ± 2.64	4.15	−6.78 ± 0.5
0.6087	37.79 ± 1.01	23.34 ± 2.34	6.94 ± 1.95	0.36	16.03 ± 3.05	3.54	−7.78 ± 0.4
0.7044	36.66 ± 0.58	19.84 ± 0.58	7.09 ± 1.92	0.29	12.46 ± 2.00	2.75	−8.97 ± 0.4
0.7932	33.60 ± 1.07	15.62 ± 2.48	7.20 ± 1.96	0.21	8.21 ± 3.16	1.91	−11.22 ± 1.3
0.9279	28.93 ± 1.37	9.31 ± 2.79	6.96 ± 2.10	0.07	2.28 ± 3.49	0.62	−26.14 ± 14.8
1.0000	28.66 ± 0.60	7.35 ± 0.80	7.35 ± 2.51	0	0	0	—

in **Table 4** and the original scattering data for all four temperatures studied is given in **Table 1**. The lines drawn are merely guides to the eye and are not the results of any data fitting. The relative magnitude of each Rayleigh ratio is easily seen. Particularly informative is the magnitude of R_C compared to R_{IS}. The scattering of mixtures appears dominated by fluctuations in concentration for $T < 300$ K but R_C becomes less of a factor for $T > 300$ K though it remains the major contributor to R_{IS}. Clearly the magnitude of R_{IS} decreases

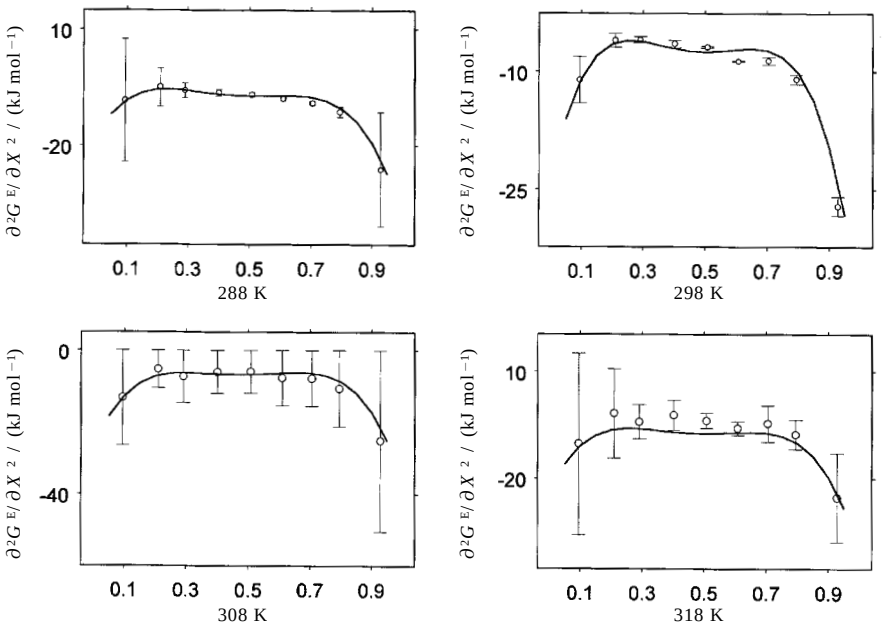

Fig.2　The second derivative of G^E with composition at the temperatures 288, 298, 308, and 318 K. Units are kJ mol^{-1}. Uncertainties were estimated by addition in quadrature of the uncertainties in the experimental factors. The solid lines result from fourth order Redlich-Kister fits to the experimental points. Composition is mole fraction of toluene.

with temperature. The biggest change with temperature is the relative magnitude of R_C compared to $R_{C,ID}$. $R_{C,ID}$ varies little in shape or magnitude with temperature but R_C varies considerably. Since it is the comparison of R_C to $R_{C,ID}$ that determines the magnitude of the excess Gibbs potential, the closer R_C is to $R_{C,ID}$, the smaller is G^E. This observation is borne out experimentally by **Fig.3** that shows G^E(318 K) to be the smallest excess Gibbs potential.

Fig.2 presents the experimental $\partial^2 G^E/\partial X^2$ data calculated via equation (16). The solid lines are the theoretical fits to a 4th order Redlich-Kister polynomial derived by differentiating a 6th order polynomial assumed for G^E. The data and the fits show no remarkable features except the expected steep downward curve near X＝0 and 1. The midrange is basically flat but the magnitudes do show a trend. The very approximate values at the midpoint of the curve are : −16 kJ mol^{-1} (288 K), −8 kJ mol^{-1} (298 K), −15 kJ mol^{-1} (308 K), and −17 kJ mol^{-1} (318 K). This trend in midrange values is mirrored in the G^E values presented in **Fig.3** as functions of temperature as G^E first increases and then decreases.

The origin of the temperature dependence of G^E

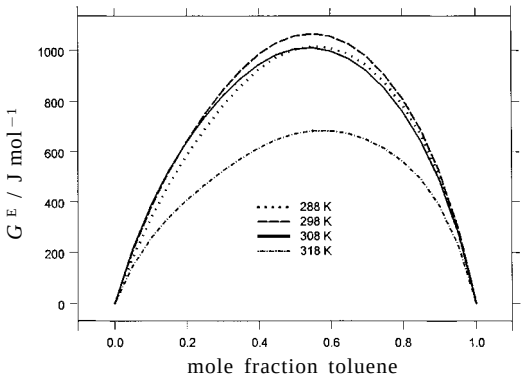

Fig.3　$G^E(T,X)$ for the temperatures 288, 298, 308, and 318 K. Units are J mol^{-1}. Composition is mole fraction of toluene. The lines result from the sixth order Redlich-Kister fits to the second derivative data shown in Fig.2.

seen in **Fig.3** can be traced back to the magnitude of the concentration fluctuation term R_C. Apparently the influence of increased temperature over-rides the influence of intermolecular forces on the concentration fluctuations.

The marked asymmetry noted in the R_{IS} and R_C

Table 5 Fitting coefficients for a sixth order Redlich-Kister expansion for G^E at the temperatures 288, 298, 308, and 318 K. The fitting equation is $G^E = X(1-X)[g_0 + g_1(1-2X) + g_2(1-2X)^2 + g_3(1-2X)^3 + g_4(1-2X)^4]$.

T /K	g_0 / J mol^{-1}	g_1 / J mol^{-1}	g_2 / J mol^{-1}	g_3 / J mol^{-1}	g_4 / J mol^{-1}
288	4015	−869	435	−489	956
298	4230	−728	462	−416	1167
308	4023	−547	609	−277	1113
318	2689	−689	431	−330	1491

plots compared to a simple parabola is not as evident in the G^E results except for the G^E(318 K) value where the asymmetry is quite noticeable. This G^E asymmetry can also be ascribed to the R_C and $R_{C,ID}$ comparison where it is noticed $R_{C,ID}$ has a maximum lying on the alcohol rich composition region while R_C has a maximum lying in the toluene rich composition region. At 318 K the location of these maximum with the relative closeness of the magnitude of each ratio, combine to broaden, almost flatten, the G^E(318 K) curve.

The excess entropy can be calculated when the excess Gibbs potential is known as a function of temperature from G^E calculated via equation (20).

$$-S^E = \left(\frac{\partial G^E}{\partial T}\right)_p \tag{20}$$

Moreover, once the excess entropy is known, the excess enthalpy can be calculated from the well known relationship $G^E = H^E - TS^E$. The trends in G^E with temperature and composition are shown as a partial T, X surface in **Fig.4**. As a function of temperature the excess Gibbs potential increases slightly, goes through a maximum at about 295 K, and then decreases. The excess functions G^E, S^E, and H^E for a equal molar mixture of propan-2-ol and and toluene are presented in **Fig.5** over the temperature range 288 to 318 K.

At low temperatures, S^E is entirely negative while at higher temperatures it is entirely positive. Below 295 K where $S^E < 0$, there is a loss in the number of ways the mixture can organize itself relative to the unmixed pure components. Above 295 K, there is a gain. This might imply some critical "structure breaking" occurs in the mixtures around 295 K.

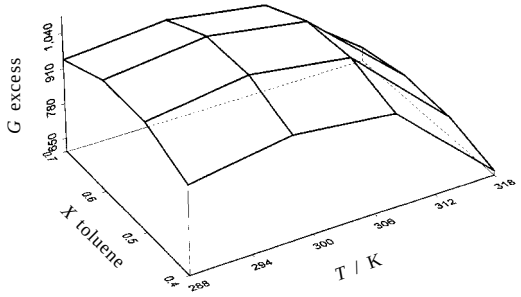

Fig.4 A $G^E(T,X)$ surface for the observed temperatures 288, 298, 308, and 318 K and the middle portion of composition $X_{toluene} = 0.4$ to 0.7. A maximum in both the temperature and composition directions is exhibited. The lines are guides to the eye joining the calculated $G^E(T,X)$ values.

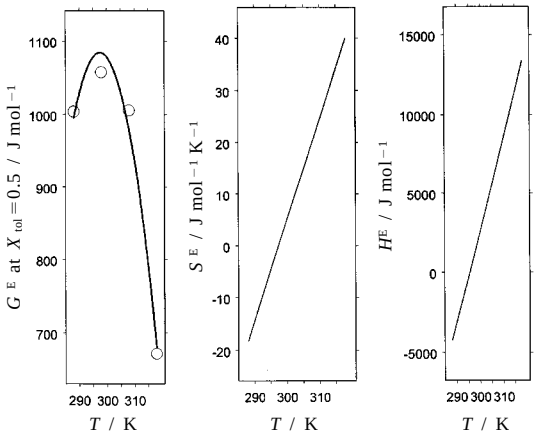

Fig.5 $G^E(T, X_{tol} = 0.5)$ fit to a quadratic in T from which S^E and H^E were derived in the temperature range of 288 to 318 K.

The H^E follows the same linear increase as S^E with the interesting prediction that H^E of mixing would be very small around 295 K. These temperature results for S^E and H^E are probably only valid in the trends they suggest and not in actual magnitudes.

11. Conclusions

The technique of Rayleigh laser light scattering can be employed to obtain G^E of binary liquid mixtures. The technique is fast and relatively simple compared to the traditional calorimetry and vapor pressure

measurements. Obtaining the data as a function of temperature also allows the S^E and H^E to be acquired easily. Binary mixtures of propan-2ol and toluene first show an increasing G^E with temperature that then decreases with temperature to suggest S^E values that are < 0 for $T < \approx 300$ K while > 0 for $T > \approx 300$ K. Around 300 K H^E is predicted to be essentially zero. All of these conclusions appear based on concentration fluctuations decreasing as temperature increases.

The convenience of this technique now should allow systematic study of mixtures of homologs to better appreciate from the data trends, the origins of non-idealities in liquid mixtures.

Acknowledgments

Financial support from the Mabel and Arnold Beckman Research Fund administered by Harvey Mudd College and from the National Science Foundation through Grant USE-8851387 for the laser equipment is here gratefully acknowledged. The authors wish to thank Professor Yatsuhisa Nagano for the invitation to present these results.

References

1) D. J. Coumou and E. L. Mackor, *Trans. Faraday* **60**, 1726-1735 (1964).
2) G. Cohen and H. Eisenberg, *J. Chem. Phys.* **43**, 3881-3887 (1965).
3) A. A. Abdel-Azim, W. Cheng, M. J. El-Hibri, and P. Munk, *J. Phys Chem.* **92**, 2663-2668 (1988).
4) W. Cheng, A. A. Abdel-Azim, M. J. El-Hibri, Q. Du, and P. Munk, *J. Phys Chem.* **93**, 8248-8253 (1989).
5) J. Cabbanes, *La Diffusin Moleculaire la Lumiere*, Les Presses Universitaires de France: Paris, Chapter X (1929).
6) M. Kerker, *The Scattering of Light*, Academic Press: New York, p.580 (1969).
7) J. P. Kratohvil and C. Smart, *J. Colloid Sci.* **20**, 875-892 (1965).
8) N. Šgudović and G. Deželić, *Croatia Chem. Acta* **45**, 385-406 (1973).
9) A. Einstein, *Ann. Phys.*(*Leipzig*) **33**, 1275 (1910).
10) N. M. D. Brown, J. F. Maguire, J. F. Swinton, *J. Chem. Thermodynamics* **10**, 855-866 (1978).
11) J. F. Eykman, *Recl Trav. Chem. Pay-Bas* **14**, 185 (1985).
12) A. A. Abdel-Azim and P. Munk, *J. Phys. Chem.* **91**, 3910-3914 (1987).
13) R. L. Schmidt and H. L. Clever, *J. Phys. Chem.* **72**, 1529-1536 (1968).
14) P. J. Flory, *J. Chem. Phys.* **9**, 660-661 (1941).
15) M. L. Huggins, *J. Chem. Phys.* **9**, 440 (1941).
16) K. Redlich and A. T. Kister, *Ind. Eng. Chem.* **40**, 345 (1948).
17) W. Kaye and J. B. McDaniel, *Applied Optics* **13**, 1934-1937 (1974).
18) B. Chu, *Laser Light Scattering*, Academic Press: New York (1991).

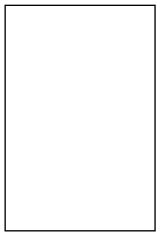

Gerald R. Van Hecke
Department of Chemistry, Harvey Mudd College, 301E. Twelfth Street, Claremont, California 91711-5990, TEL. +1-909-607-3935, FAX. +1-909-607-7577, e-mail: Gerald_VanHecke@hmc.edu

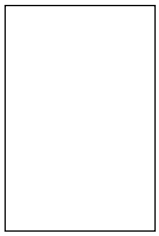

Robert A. Westervelt
Department of Chemistry, Harvey Mudd College, 301E. Twelfth Street, Claremont, California 91711-5990